Curb-intersection feature based Monte Carlo Localization on urban roads

Citation: Qin, B., Z. J. Chong, T. Bandyopadhyay, M. H. Ang, E. Frazzoli, and D. Rus. "Curb-intersection feature based Monte Carlo Localization on urban roads." In 2012 IEEE International Conference on Robotics and Automation, 2640-2646. Institute of Electrical and Electronics Engineers, 2012.

As Published: http://dx.doi.org/10.1109/ICRA.2012.6224913

Publisher: Institute of Electrical and Electronics Engineers (IEEE)

Persistent URL: http://hdl.handle.net/1721.1/81465

Version: Author's final manuscript: final author's manuscript post peer review, without publisher's formatting or copy editing

Curb-Intersection Feature Based Monte Carlo Localization on Urban Roads

B. Qin*, Z. J. Chong*, T. Bandyopadhyay‡, M. H. Ang Jr.*, E. Frazzoli§‡, D. Rus§‡

* National University of Singapore, Kent Ridge, Singapore

‡ Singapore-MIT Alliance for Research and Technology, Singapore

§ Massachusetts Institute of Technology, Cambridge, MA., USA.

***Abstract*— One of the most prominent features on an urban road is the curb, which defines the boundary of a road surface. An intersection is a junction of two or more roads, appearing where no curb exists. The combination of curb and intersection features and their idiosyncrasies carry significant information about the urban road network that can be exploited to improve a vehicle's localization. This paper introduces a Monte Carlo Localization (MCL) method using the curb-intersection features on urban roads. We propose a novel idea of "Virtual LIDAR" to get the measurement models for these features. Under the MCL framework, above road observation is fused with odometry information, which is able to yield precise localization. We implement the system using a single tilted 2D LIDAR on our autonomous test bed and show robust performance in the presence of occlusion from other vehicles and pedestrians.**

I. Introduction

Intelligent Vehicle/Highway Systems (IVHS) have been one of the most popular research areas in robotics. By realizing autonomous navigation, intelligent vehicles enhance operational safety and efficiency of the transportation system. Localization is one fundamental requirement for vehicle autonomy. This paper investigates the ability to localize under minimal sensing, with only one LIDAR, odometry information and prior road network information.

In the past few years, researchers spent much effort on the fusion of Global Positioning System (GPS) and Inertial Navigation System (INS) to estimate vehicle position[12], [13], [3]. This approach usually achieves good accuracy in open areas; however, the performance deteriorates in dense urban environment, where GPS signal quality gets severely undermined by satellite blockage and urban multipath propagation due to high buildings, as discussed in [11]. To overcome this problem, road-matching method can be used. The basic idea underlying road-matching is to treat road constraint of vehicle motion as observation. The road is perceived as a line segment, with no lane width information. By checking the on-driving road segment with a road-map, additional localization information can be derived. In [5], Najjar et al. propose a road-matching localization algorithm, using Belief Theory for road selection and Kalman Filtering for recursive estimation. Some other similar studies can be found in [7], [6]. These road-matching algorithms achieve good localization in a global fashion. However, they are not designed to generate accurate position relative to the road. In this sense, the localization is at a coarse level, which may be inadequate for a vehicle performing complex tasks on road surface.

In other studies, researchers refer to local features for high precision localization. In [14], lane markers are extracted to reduce localization error. But due to the fact that lane makers just carry lateral position information, longitudinal localization error can be reduced only when the road curvature is big. In [8], a novel "Virtual 2D Scans" method is proposed by making use of the building outlines as features. A simplified 2D line feature map is generated beforehand as prior knowledge. However, possible lack of building features and slow update rate limits its effectiveness.

One of the most dominant features on an urban road is the curb. Serving as the road boundary, curb features carry much richer localization information than lane markers. In [9], [2], single side curb features are extracted by a vertical LIDAR to improve vehicle localization together with road information. While these algorithms reduce lateral localization error considerablely, they help little in the longitudinal direction. Intersection features appear at junctions of roads, where no curb exists. While curb features mostly help localize vehicle laterally in the road, intersection features carry rich longitudinal information. The combination of curb and intersection features gives a complete picture of the urban road network. The complementary nature of these two kinds of features makes it well suited to improve the vehicle localization.

This paper proposes a Monte Carlo Localization (MCL) method using the curb-intersection feature on urban roads. Our main contribution is to propose a novel idea of "Virtual LIDAR", where curb and intersection measurements are utilized to improve localization accuracy laterally and longitudinally. This paper adopts the MCL framework to fuse odometry information with road observation, which is able to yield precise pose estimation. We implement the system using a single tilted 2D LIDAR to detect the curb-intersection features and show robust performance in the presence of occlusion from other vehicles and pedestrians.

The remainder of this paper is organized as follows. In Section II, the extraction of curb and intersection features is introduced. Section III provides details of the curb-intersection based MCL method. Experimental results and analyses are presented in Section IV. Finally, Section V concludes the paper and discusses future work.

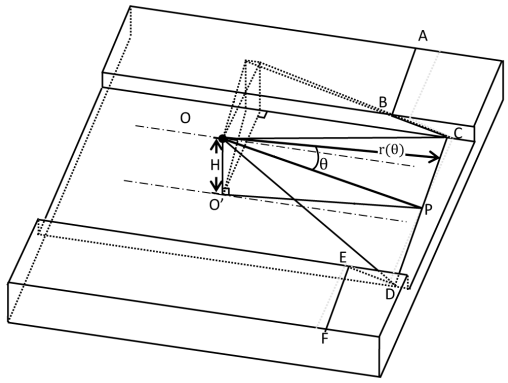

Fig. 1. Model of LIDAR Sensing On Road

II. Curb-Intersection Feature Extraction

There are numerous studies for the detection of road boundary. One of the ways is to utilize a tilted-down LIDAR for curb detection. Cramer et al. [4] applied Hough Line for scan segmentation and feature extraction, while Kodagoda et al. [16], [10] achieved the same goal by using EKF filter. This paper presented an intuitive two-step method to detect both curb and intersection, which proves to be efficient and robust. Similar work can be found in [17].

A. Segmentation of Laser Scan

In the first step, one single laser scan is segmented into several pieces, by virtue of its typical laser range/angle characteristics on road. Fig. 1 shows the model of sensing on road. One LIDAR sensor is mounted at point O, with its laser beam angle as θ. The distance between point P and O' is the look-ahead distance of the tilted-down LIDAR. As presented in Fig. 1, laser beams from point O are cast onto different planes, i.e. road surface plane, curb plane, road shoulder plane, and so on. From this model, a piecewise function can be derived to represent the relationship between the beam angle and range value, with each interval corresponding to an individual plane. Without involving too many details, a simplified formula can be represented as:

$$r(\theta) = \begin{cases} \dots & \dots & \dots \\ R_{leftCurb}(\theta) & \text{for} & \theta_C \le \theta \le \theta_B \\ R_{roadSurf}(\theta) & \text{for} & \theta_D \le \theta \le \theta_C \\ R_{rightCurb}(\theta) & \text{for} & \theta_E \le \theta \le \theta_D \\ \dots & \dots & \dots \end{cases} \quad (1)$$

Due to the piecewise fact of function $r(\theta)$, a second-order differential filter can be implemented to detect the edges:

$$r_f(\theta) = \sum_{i=-5}^{i=-3} r(\theta + i \times \mu) + \sum_{i=3}^{i=5} r(\theta + i \times \mu) - \sum_{i=-2}^{i=0} r(\theta + i \times \mu) - \sum_{i=0}^{i=2} r(\theta + i \times \mu) \quad (2)$$

where μ is angular resolution of the LIDAR sensor, and $\theta \in [-\pi/2 + 5\mu, \pi/2 - 5\mu]$. Boundary points are extracted as local maxima or minima in the filter response plot, and their values should exceed certain threshold, as shown in Fig. 2.

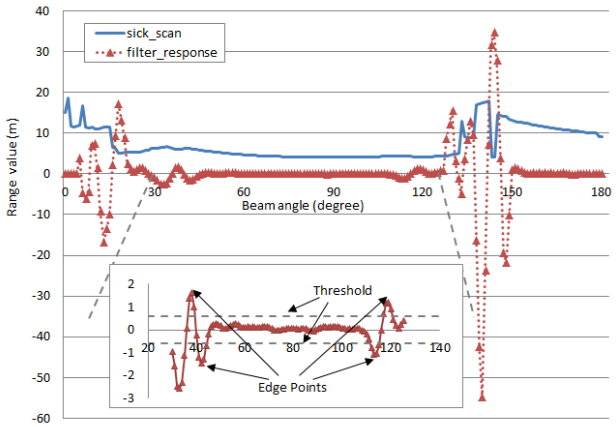

Fig. 2. Raw LIDAR Reading and Filter Response

B. Classification of Scan Segments

In the second step, scan segments generated are fed into a sequential classification process.

1) Road surface segment, shown as line CD in Fig. 1, is selected first. It always locates between two edge points nearest to center of the sensor.
2) Curb lines, (BC and DE of Fig. 1), are searched subsequently, based on point C and D determined from the former step.
3) Rest segments are other features off the road.

Some restrictive criteria are applied during above steps, such as road width, curb height, etc. Specifically, to extract a valid curb feature, the length of segment CD should be bigger than the minimum value of road width, the curb height of segment BC (or DE) should be within certain range, and the number of laser beams on BC (or DE) should be over certain threshold, etc. Only when all these criteria get satisfied, classification result is thought to be valid. Thus most noise like vehicles and pedestrians get filtered. One typical classification result is shown in Fig. 3. Among these categories, curb is saved for further usage.

It should be clarified that, a fixed maximum detection range is defined for the curb extraction algorithm. If the distance of curb edge (C or D), to projected center O' equals to or exceeds this range, the curb features are deemed unreliable, and will yield "no-curb" result. For this reason, above algorithm doesn't apply to situations at intersection, where curb is too far away, or there may be no curb at all. However, the fact of "no-curb" also carries useful localization information. To embody this kind of information, a virtual "intersection feature" is introduced.

As shown in Fig. 4, intersection feature is represented by a virtual beam $\overrightarrow{PR}$ (or $\overrightarrow{PL}$), with its direction tangent to $\overrightarrow{O'P}$ and distance as maximum detection range of curb extraction. It should be clarified that feature extraction of left and right sides are independent, enabling both curb and intersection

feature extraction at a T-junction. Implementation of using curb-intersection features for Monte Carlo Localization will be discussed in Section III.

III. Monte Carlo Localization Algorithm

A. MCL Overview

In this paper, Monte Carlo Localization (MCL) is applied to estimate the vehicle pose. MCL is a probabilistic localization algorithm based on Bayes' Theorem and Monte Carlo method. A thorough study is made by Sebastian Thrun et al [15]. The belief $bel(x_t)$ in MCL is represented by a set of M particles $x_t^{[m]}$, and each particle is paired with an importance weight $w_t^{[m]}$:

$$bel(x_t) \sim \{x_t^{[m]}, w_t^{[m]}\}_{m=1}^{M} \tag{3}$$

MCL estimates the position of the vehicle recursively by repeating the following steps:

1) Prediction: a new set of particles $\{x_t^{[m]}, w_t^{[m]}\}_{m=1}^{M}$ for time t is generated with $\{x_{t-1}^{[m]}, w_{t-1}^{[m]}\}_{m=1}^{M}$ and the control u^t, according to certain motion model $p(x_t|u_t, x_{t-1})$.
2) Correction: the importance weight of each particle in $\{x_t^{[m]}, w_t^{[m]}\}_{m=1}^{M}$ is adjusted with new measurements z^t, according to certain measurement model $p(z_t|x_t, m)$.
3) Resampling: the particle set $\{x_t^{[m]}, w_t^{[m]}\}_{m=1}^{M}$ will be resampled when necessary. After resampling, the distribution of the particles approximates $bel(x_t)$.

B. Pseudo-3D Odometry Motion Model

In prediction step, a motion model is applied to propagate particles for prior belief distribution $\overline{bel}(x_t)$. Generally, a 2D motion model in [15] is enough. Even for a vehicle moving in 3D world, we solve the localization problem on its horizontal projection plane, as shown in Fig. 5. Here we extend the 2D motion model to a Pseudo-3D one, by introducing a pitch noise part.

Table I represents the Pseudo-3D Odometry Sample Motion Model. This model is used for sampling from $p(x_t|u_t, x_{t-1})$ with relative motion information on the horizontal plane. Here γ denotes the pitch angle, δ_{rot1} the initial rotation on the projected plane, δ_{trans} the translation and δ_{rot2} the second rotation. More details can be found in [15].

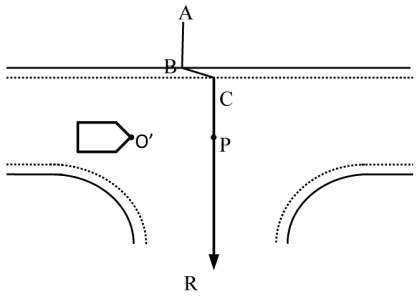

Fig. 4. Curb-Intersection Feature at a T-junction

TABLE I
Pseudo-3D Odometry Sample Motion Model (u_t ,x_{t-1})

1. $\hat{\delta}_{rot1}$	$= \delta_{rot1} - sample(\alpha_1\delta_{rot1}^2 + \alpha_2\delta_{trans}^2)$
2. $\hat{\delta}_{trans}$	$= \delta_{trans} - sample(\alpha_3\delta_{trans}^2 + \alpha_4\delta_{rot1}^2 + \alpha_4\delta_{rot2}^2 + \alpha_5\gamma^2\delta_{trans}^2)$
3. $\hat{\delta}_{rot2}$	$= \delta_{rot2} - sample(\alpha_1\delta_{rot2}^2 + \alpha_2\delta_{trans}^2)$
4. x'	$= x + \hat{\delta}_{trans}\cos(\theta + \hat{\delta}_{rot1})$
5. y'	$= y + \hat{\delta}_{trans}\sin(\theta + \hat{\delta}_{rot1})$
6. θ'	$= \theta + \hat{\delta}_{rot1} + \hat{\delta}_{rot2}$
7. $return\ x_t$	$= (x', y', \theta')^T$

C. Curb-Intersection Measurement Model

In correction step, importance weights of particles get adjusted based on measurements and related sensor models. Here we propose a novel idea of "Virtual LIDAR" to obtain the required models.

a) Virtual LIDARs on Horizontal Plane: As discussed in previous sections, measurements extracted here are curb segments (line BC and DE), or virtual beams ($\overrightarrow{PR}$ and $\overrightarrow{PL}$). However, because curb-intersection features are extracted using a tilted-down LIDAR, building its measurement model is not an easy task. To simplify computation, we try to solve the problem on 2D horizontal plane (z=0), as illustrated by Fig. 6.

For curb features, segments BC and DE are projected as

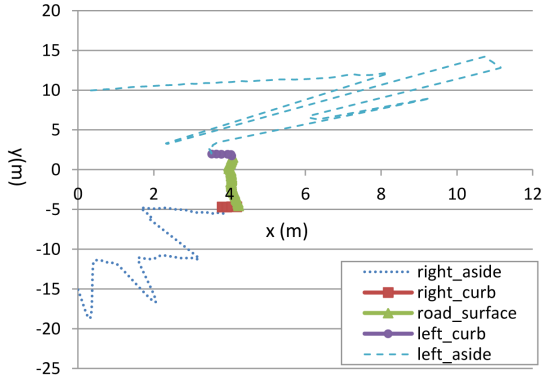

Fig. 3. Road features classification

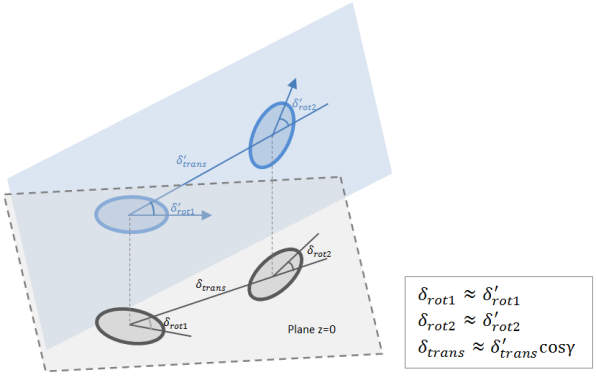

Fig. 5. Pseudo-3D Localization

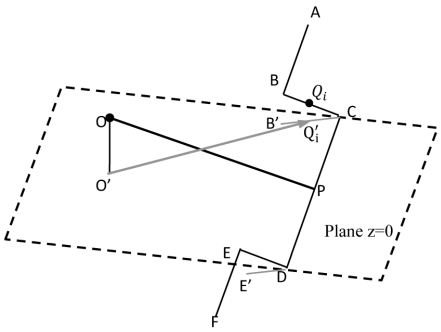

Fig. 6. Virtual laser beams

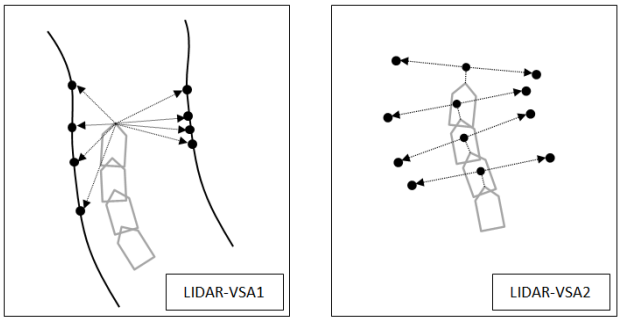

Fig. 7. Assembled Virtual LIDARs

$B'C$ and DE'. Let Q_i be a random point on BC (or DE), and its image on $B'C$ is Q_i'. A virtual laser beam can be conceived of as $\overrightarrow{O'Q_i'}$. In this way, a virtual planar LIDAR (LIDAR-V1), centered at O' can be built. This LIDAR is somehow exotic: it can only see curb lines, and its beam angle is not evenly spaced. The full scale range of this virtual LIDAR is the maximum detection range for curb. With similar ideas, LIDAR-V2 centered at P can be modeled for intersection features. LIDAR-V2, different from LIDAR-V1, have at most two virtual beams, $\overrightarrow{PR}$ and $\overrightarrow{PL}$, with its range values always the maximum detection range for curb.

b) Scan-Assembled Virtual LIDARs: With two virtual LIDARs established, the MCL problem using curb-intersection feature is reduced to a common MCL problem with planar LIDARs. However, because scans of the virtual LIDARs carry much sparser information than real ones, it is advisable to assemble several scans at different time into one. The assumption validating this operation is odometry remains accurate within a short distance interval. The new assembled virtual scan can then be treated as a real scan, and fed into the MCL processing.

During the scan assembling of LIDAR-V1, to reduce computational cost, only two curb points (C and D) are retained for each scan. Curb points recorded at different time are then translated into the latest LIDAR coordinate, serving as endpoints of virtual laser beams casted from a new virtual LIDAR, denoted as LIDAR-VSA1. As for LIDAR-V2, two virtual beams are recorded at different time, together with their casting origins. The new virtual assembled LIDAR is even more exotic: it is composed of several 2-beam range finders, with each finder mounted at different positions and angles. When the beam number of LIDAR-VSA1 (or LIDAR-VSA2) exceeds certain "Assembling Threshold", one virtual measurement is published. Finally, we get two new virtual LIDARs: LIDAR-VSA1 for curb feature, and LIDAR-VSA2 for intersection feature, as shown in Fig. 7

c) Measurement Model: The measurement model is used to adjust the importance weight of each factor. It is formally defined as a conditional probability distribution $p(z_t|x_t, m)$, where x_t denotes the robot pose, z_t denotes the measurement at t, and m is the map of the environment, according to [15]. In our algorithm, z_t is curb and intersection features, and m is an occupancy grid map of road boundary. By applying the idea of "Virtual LIDAR", the curb-intersection feature is converted into virtual laser scan, which permits us of using common LIDAR models for the measurement.

LIDAR-VSA1 (for curb feature) adopts "Likelihood Field Range Finder Model", considering its computational efficiency and less sensitivity to noise. However, LIDAR-VSA2 (for intersection feature) has to adopt "Beam Range Finder Model" due to its working manner. As mentioned in previous parts, intersection feature is represented by a set of virtual beams with maximum range values, meaning that no curb is met along their virtual light path. Only through ray tracing in "Beam Model" can this working manner gets properly interpreted.

D. Practical Considerations

a) MCL Estimation Frequency: In this paper, MCL estimation loop is triggered by the arrival of virtual measurements. Whenever an assembled virtual scan from "LIDAR-VSA1" or "LIDAR-VSA2" is available, prediction step is performed in a retrospect manner, followed by a correction step with the new incoming measurement. In this sense, the frequency of virtual scan is quite important. To control the frequency of "LIDAR-VSA1" and "LIDAR-VSA2", we can either control the frequency of curb-intersection feature extraction, or control their "Assembling Threshold". We find it is always advisable to obtain curb-intersection feature when the vehicle moves, and suspend the process when stopping. "Assembling Threshold" is determined by trading off MCL response speed and robustness.

b) Algorithm Robustness: The robustness of MCL is one of key issues. A reasonably big "Assembling Threshold" will help the algorithm to resist measurement noise. Actually, before curb-intersection is fed into MCL, we adopt the temporal EKF method in [16] to reduce measurement noise. The temporal filter is applied after curb extraction and before scan assembling operation. In the filter update step, if the Mahalanobis distance between the detected curb and the predicted one exceeds certain threshold, the newly detected curb will be considered as noise and discarded. This EKF method helps to eliminate minor noise like pedestrians and small cars.

Fig. 8. Yamaha G22E golf cart mounted with various sensors

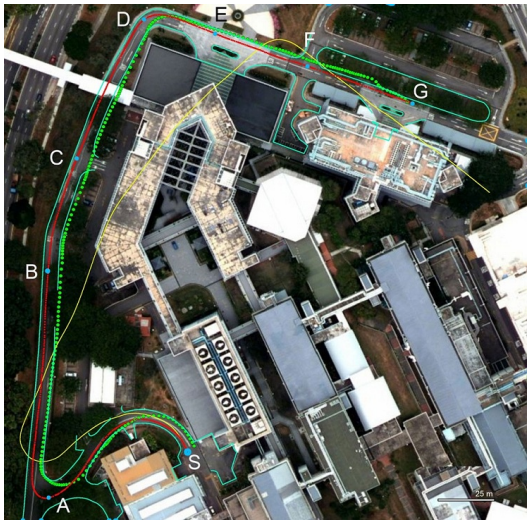

Fig. 9. Localization Results

Another strategy that we apply to increase algorithm robustness is the injection of random particles in [15]. When the vehicle is locally lost or the measurement is badly corrupted for sometime, the short-term average of particle importance factors will be decreased remarkably. In this case, a fraction of particles will be generated around the predicted position, and spread according to a uniform distribution within certain range.

c) Map-Incorporated Prediction: For vehicle localization on urban roads, one assumption is that vehicles are not likely to drive off-road. This assumption allows us to penalize those erratic particles by decreasing their weight importance. In this way, map information is also incorporated into the prediction step, which makes our localization more robust.

IV. Experiments

A. Experimental Setup

Our test bed is a Yamaha G22E golf cart with various sensors, as shown in Fig. 8. We use one SICK LMS 291 LIDAR for curb and intersection detection. It is mounted in the front, with a tilted-down angle of 18 degrees. One wheel encoder (Scancon-2RS) and one IMU (3DM-GX3-25) are mounted on the cart provide necessary odometry information (distance, pitch and yaw). The proposed algorithm is tested online. In the experiment, the golf cart is driven manually on a hilly road at the campus of National University of Singapore, from point S to G, as shown in Fig. 9. Several big slopes are involved along the way, with the maximum height difference over 10 meters. The average speed in test is about 3.5 m/s. The reference road map is an occupancy grid map manually generated from a vector-format road map provided by Land Transport Authority (LTA) of Singapore and satellite map. The size of this road map is 200 meter by 240 meter, with grid resolution of 0.1 meter, as shown by Fig. 10.

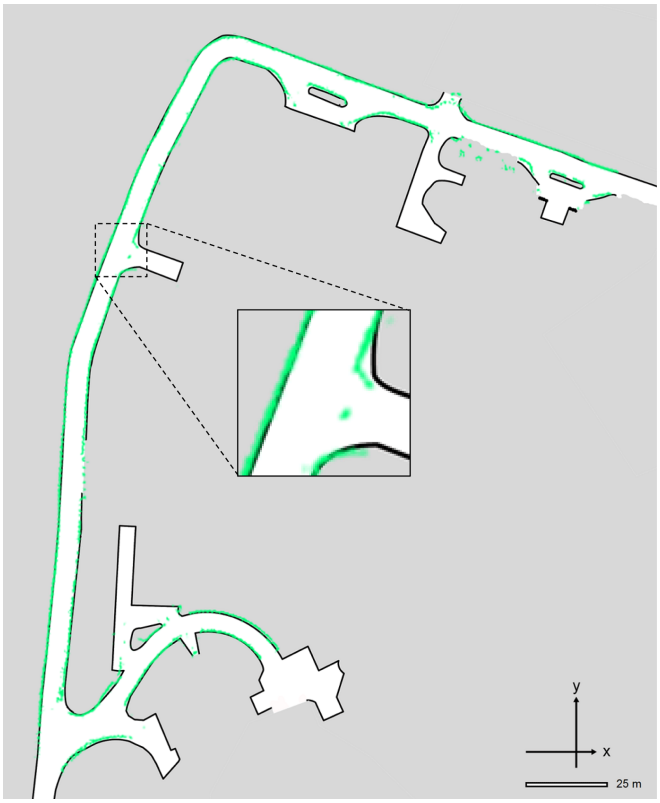

Fig. 10. Road boundary map and detected curb features

B. Experimental Results

In the test, the golf cart is given a rough initial position at S, and driven for about 430 meters to G. The localization results are shown in Fig. 9. The light-blue lines denote road boundary. The red line marks the localization result of the curb-intersection feature based MCL, and raw odometry trace is shown by yellow line. For comparison, we also give the localization result from one state of art GPS/INS module (Ublox EVK-6R) by green dotted line. From Fig. 9, it is apparent that dead-reckoning odometry drifts a lot after certain distance. Even when it is fused with GPS, INS/GPS trajectory tends to fall out of road boundary. Because our

algorithm incorporates road surface information, it helps to correct the odometry and yield fairly decent estimation. Fig. 10 shows the occupancy grid map of road boundary. The green points represent the curb features detected in the experiment, overlaid on top according to localization results. Some unexpected points in the figure are measurement noise.

To evaluate the localization result, estimation errors of position and attitude are calculated against ground truth values. We rely on our occupancy grid map to get the ground truth. When the ground truth is needed, vehicle position relative to the road network is measured carefully and marked onto the map image. By counting the pixel in the image, the ground truth can be calculated easily. The vehicle was driven manually to the selected points marked in Fig. 9 and the errors in location estimate are plotted in Table II. It can be seen that position error of our algorithm is usually small, less than 0.6 meter; and the orientation estimation is quite accurate, less than 3 degrees to the ground truth.

From Table II, one can also observe that position errors at some critical points of intersections and turnings (like A, C, D, F) are much smaller than that of the straight road (like B). The phenomena can be explained from the estimated variance of particles. Fig. 11 shows "estimation variance" vs "driving distance" in road longitudinal and lateral direction. During the whole test, lateral estimation variance remains small, which means particles are confident about the lateral position. However, the longitudinal variance changes remarkably along the drive, which determines the accuracy of localization.

During the trip from A to B, the longitudinal variance increases first, due to consistency of road boundary. When the road represents a small curvature, curb features embodying this information will reduce the longitudinal variance. Thanks to the look-ahead distance of the tilted-down LIDAR,

TABLE II

LOCALIZATION ERROR AT SEVERAL MARKED POINTS

Marked Points	A	B	C	D	E	F	G
Position Error (m)	0.20	0.55	0.06	0.20	0.32	0.06	0.08
Orientation Error (deg)	< 3						

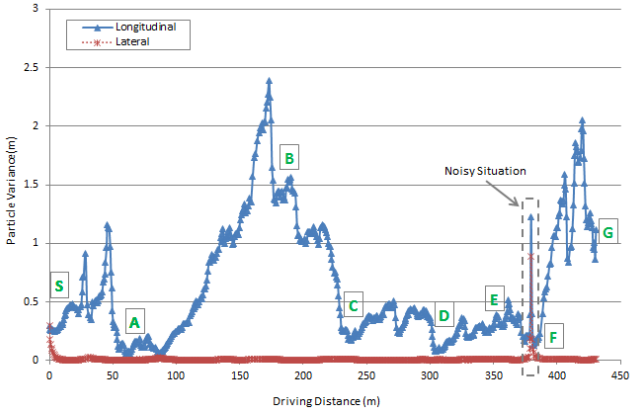

Fig. 11. Position estimation variance

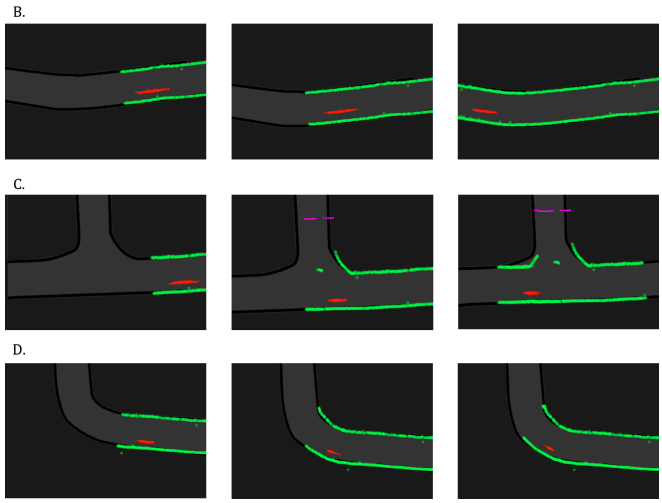

Fig. 12. Typical particle behaviours near some marked points in Fig. 9

the vehicle will sense this information before it actually arrives there. When the vehicle is approaching the intersections and turnings (like A, C, D, F), the particles are condensed significantly by the detected intersection and the tightly curved curb features. The longitudinal variance at these points is usually less than 0.4 meter. Hereby it can be concluded that, while curb features on straight roads help to estimate the lateral position, the intersection and tightly curved curb features contribute very much to the longitudinal positioning. Fig. 12 shows typical particle behaviours around point B, C, D. The red arrays are particles, with green lines as detected curbs, and purple segments to visualize intersection features.

In the experiment, there is one situation where measurement noise becomes severe: when the vehicle is passing by an intersection at F. As mentioned in Section III, injection of random particles is performed to overcome this "noisy situation". This operation leads to an increase of the estimation variance, as reflected in Fig. 11. As long as new reliable measurements come in, particles quickly converge, and localization quickly recovers from the bad situation. Actually, although light measurement noise happens from time to time in the test, the localization is hardly disturbed. The robustness of this algorithm is proved.

Besides the manual drive, we conducted another simple semi-autonomous drive to test our localization algorithm. The vehicle is required to navigate from point S to G by following a predefined route. While the throttle and brake are controlled manually, the steering is controlled by an onboard computer. It turns out that the localization is accurate enough for the vehicle to reach its target smoothly.

C. Autonomous System Demonstration

As a part of the overall goal of attaining mobility on demand, we conducted an autonomous system demonstration in July 2011, where we had guests request the vehicle to navigate from a pickup location to pre-specified drop-off locations shown in Fig. 13. More details and videos of the oper-

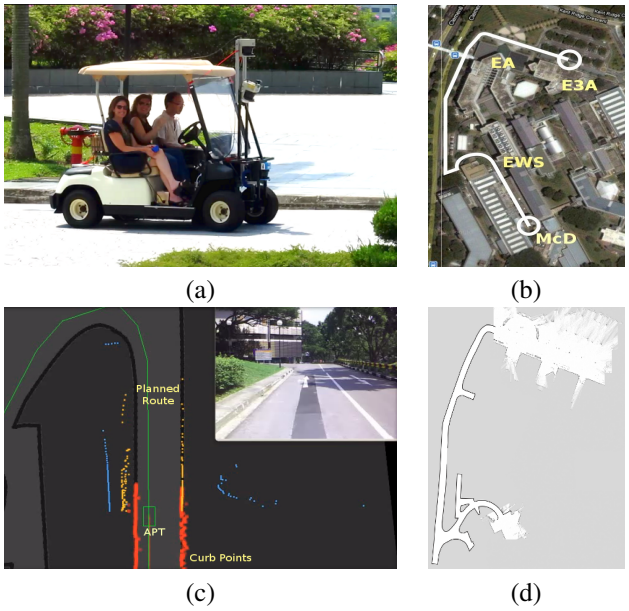

(a) (b) (c) (d)

Fig. 13. Autonomous system demonstration: (a) Vehicle in operation, (b) Pickup-Dropoff points, (c) Snapshot of curb localization estimate, (d) curb map augmented by planar patches

ation can be found at (http://web.mit.edu/tirtha/Public/demo-web/golfcart.html) [1].

The autonomous vehicle localization was performed in July 2011 purely using curb-only road features. At the pickup and drop-off points where few curb features exist, patches of 2-D occupancy planar maps were augmented to the road network map. An secondary planar LIDAR sensor readings were incorporated to acheive higher accuracy in localization at these critical points. During the course of the demonstration, the autonomous vehicle serviced almost 10 requests from the guests, running over 7 km and the curb-only localization failed at an inclined T-junction 2 times over the whole demo. The reason for failure was determined to be lack of curb features and planar maps at the intersections and T-junctions, which prompted us to include such intersection features resulting in the localization scheme presented in this paper. Since then till date we have covered over 50km in autonomous runs during various demonstrations with onboard passengers without the localization failing in any segment of the route. This included situations where the curb detection was hampered briefly by traffic. However such events were detected as no-information case and recovered from once the sensory occlusion was overcome.

V. Conclusions and Future Work

This paper proposes a Monte Carlo Localization algorithm based on the curb-intersection feature, which is extracted through a two-step procedure. A novel idea of "Virtual LIDAR" is applied to get the measurement models. An occupancy grid map for road boundary is used as prior knowledge. From experiment results, our algorithm proves to be accurate and robust. Although the longitudinal estimation variance may increase at a long straight road, it will not influence much the control of vehicle motion. The look-ahead distance in the feature extraction can help vehicles to localize accurately before they reach crossings and turnings.

One disadvantage that limits the proposed algorithm is its reliance on an occupancy grid map. It is laborious to generate this map manually, and its storage is also not efficient. We plan to substitute the occupancy grid map with a vector map. In future work, other features of urban roads like lane markings will also be exploited for better localization.

References

[1] "Autonomous Personal Transporter (APT) : Demo July'11." [Online]. Available: http://web.mit.edu/tirtha/Public/demo-web/golfcart.html

[2] P. Bonnifait, M. Jabbour, and V. Cherfaoui, "Autonomous Navigation in Urban Areas using GIS-Managed Information," *International Journal of Vehicle Autonomous Systems*, vol. 6, no. 1/2-2008, pp. 83–103, 2008.

[3] H. Carvalho, P. DelMoral, A. Monin, and G. Salut, "Optimal nonlinear filtering in GPS/INS integration," *IEEE Transactions on Aerospace and Electronic Systems*, vol. 33, no. 3, pp. 835–850, 1997.

[4] H. Cramer and G. Wanielik, "Road border detection and tracking in non cooperative areas with a laser radar system," in *Proceedings of German Radar Symposium*, 2002, pp. 24–29.

[5] M. E. El Najjar and P. Bonnifait, "A road-matching method for precise vehicle localization using belief theory and Kalman filtering," *Autonomous Robots*, vol. 19, no. 2, pp. 173–191, 2005.

[6] C. Fouque, P. Bonnifait, and D. Betaille, "Enhancement of global vehicle localization using navigable road maps and dead-reckoning," *2008 IEEE/ION Position, Location and Navigation Symposium, Vols 1-3*, pp. 999–1004, 2008.

[7] J. Guivant and R. Katz, "Global urban localization based on road maps," *2007 IEEE/RSJ International Conference on Intelligent Robots and Systems, Vols 1-9*, pp. 1085–1090, 2007.

[8] M. Hentschel, O. Wulf, and B. Wagner, "A GPS and Laser-based Localization for Urban and Non-Urban Outdoor Environments," *2008 IEEE/RSJ International Conference on Robots and Intelligent Systems, Vols 1-3, Conference Proceedings*, pp. 149–154, 2008.

[9] M. Jabbour and P. Bonnifait, "Global localization robust to GPS outages using a vertical ladar," *2006 9th International Conference on Control, Automation, Robotics and Vision, Vols 1- 5*, pp. 1013–1018, 2006.

[10] K. R. S. Kodagoda, W. S. Wijesoma, and A. P. Balasuriya, "CuTE: Curb tracking and estimation," *IEEE Transactions on Control Systems Technology*, vol. 14, no. 5, pp. 951–957, 2006.

[11] T. Kos, I. Markezic, and J. Pokrajcic, "Effects of multipath reception on GPS positioning performance," in *ELMAR, 2010 PROCEEDINGS*. IEEE, 2010, pp. 399–402.

[12] A. Mohamed and K. Schwarz, "Adaptive Kalman filtering for INS/GPS," *Journal of Geodesy*, vol. 73, no. 4, pp. 193–203, 1999.

[13] H. H. Qi and J. B. Moore, "Direct Kalman filtering approach for GPS/INS integration," *IEEE Transactions on Aerospace and Electronic Systems*, vol. 38, no. 2, pp. 687–693, 2002.

[14] N. Suganuma and T. Uozumi, "Precise position estimation of autonomous vehicle based on map-matching," in *Intelligent Vehicles Symposium (IV), 2011 IEEE*. IEEE, pp. 296–301.

[15] S. Thrun, W. Burgard, and D. Fox, *Probabilistic robotics*. MIT Press, 2005.

[16] W. S. Wijesoma, K. R. S. Kodagoda, and A. P. Balasuriya, "Road-boundary detection and tracking using ladar sensing," *IEEE Transactions on Robotics and Automation*, vol. 20, no. 3, pp. 456–464, 2004.

[17] W. Zhang, "LIDAR-based road and road-edge detection," in *Intelligent Vehicles Symposium (IV), 2010 IEEE*, pp. 845–848.